agriculture

MDPI

Article

Simulation Parameter Calibration and Experimental Study of a Discrete Element Model of Cotton Precision Seed Metering

Shenghe Bai [1,2], Yanwei Yuan [1,2,*], Kang Niu [2], Liming Zhou [2], Bo Zhao [2], Liguo Wei [2], Lijing Liu [1,2], Shi Xiong [1,2], Zenglu Shi [3], Yihua Ma [2], Yuankun Zheng [1,2] and Gaoyong Xing [1,2]

[1] College of Engineering, China Agricultural University, Beijing 100083, China; baishenghe@caams.org.cn (S.B.); liulijing@caams.org.cn (L.L.); xiongshi@caams.org.cn (S.X.); zhengyuankun@caams.org.cn (Y.Z.); xinggaoyong@caams.org.cn (G.X.)

[2] The State Key Laboratory of Soil, Plant and Machine System Technology, Beijing 100083, China; niukang@caams.org.cn (K.N.); zhouliming@caams.org.cn (L.Z.); zhaobo@caams.org.cn (B.Z.); weiliguo@caams.org.cn (L.W.); mayihua@caams.org.cn (Y.M.)

[3] College of Mechanical and Electrical Engineering, Xinjiang Agricultural University, Urumqi 830052, China; b20213070561@cau.edu.cn

* Correspondence: yyw@caams.org.cn; Tel.: +86-135-2232-6652

Abstract: To improve the accuracy of the parameters used in the discrete element simulation test, this study calibrated the simulation parameters of cotton seeds by combining a physical test and simulation test. Based on the intrinsic parameters used for the physical test of cotton seed, according to the freefall collision method, inclined plane sliding method, and inclined plane rolling method, the contact parameters of cotton seeds and cotton seeds, stainless steel, and nylon were measured, respectively. The physical test of the accumulation angle and angle of repose of the cotton seeds was conducted. It was obtained to process the image of the seed pile with Matrix Laboratory software. The Plackett–Burman test was used to screen the significance of the simulation parameters. The optimal value range of the significant parameters was determined according to the steepest climbing test. The second-order regression model of the significant parameters, the stacking-angle error, and the angle-of-repose error were obtained according to the Box–Behnken design test. Taking the minimum stacking-angle error and angle-of-repose error as the optimization target values, the following optimal parameter combination was obtained: the interspecies collision recovery coefficient was 0.413, the interspecies static friction coefficient was 0.695, and the interspecies rolling friction coefficient was 0.214. Three repetitive simulation experiments were conducted to prove the reliability of the calibration results. The research results can be used for discrete element simulation experiments for cotton precision seed metering.

Keywords: parameter; stacking angle; angle of repose; discrete element; seeding; cotton seeds

check for updates

Citation: Bai, S.; Yuan, Y.; Niu, K.; Zhou, L.; Zhao, B.; Wei, L.; Liu, L.; Xiong, S.; Shi, Z.; Ma, Y.; et al. Simulation Parameter Calibration and Experimental Study of a Discrete Element Model of Cotton Precision Seed Metering. *Agriculture* **2022**, *12*, 870. https://doi.org/10.3390/agriculture12060870

Academic Editor: Jacopo Bacenetti

Received: 11 April 2022
Accepted: 9 June 2022
Published: 16 June 2022

Publisher's Note: MDPI stays neutral with regard to jurisdictional claims in published maps and institutional affiliations.

Copyright: © 2022 by the authors. Licensee MDPI, Basel, Switzerland. This article is an open access article distributed under the terms and conditions of the Creative Commons Attribution (CC BY) license (https://creativecommons.org/licenses/by/4.0/).

1. Introduction

As an important economic crop and fine chemical raw material in China, cotton is widely grown and is the second-largest crop after grain. In 2020, national cotton planting was about 3,168,900 hm^2, and the output was about 5,910,500 tons. It is also a key strategic material related to the national economy and people's livelihoods; cotton has good development prospects in Chinese agricultural production [1–3]. To improve the production level and economic benefits of domestic cotton, the sowing link is the most important, since it directly affects the yield and quality of cotton, and determines the level of mechanization in the subsequent operations [4,5].

Cotton precision planters can save labor, save seeds, and improve operation efficiency. They are an important way to realize mechanized cotton planting. As the core component of the cotton precision planter, the seed metering performance directly affects the operation level of the seeder [6]. At present, the vertical disc seed metering device is widely used due to its compact structure and convenient maintenance, but problems persist, such as poor seed-filling performance and a high damage rate [7–9]. Therefore, to greatly improve the planting level of cotton, scholars have carried out research on cotton high-speed precision seed-metering devices. Research shows that the main reason for seed fragmentation caused by the vertical disc seed-metering device is the friction force and shear force generated when the seed-collecting disc rotates. The movement characteristics of the seed population have an important influence on the seed-filling performance of the seed-metering device. Improving the seed-filling performance of the seed-filling area is critical to improving the performance of the seed-metering device. During the seed-filling process, however, extrusion, collision, and dragging occur between the seeds, which may easily cause replay or missed seeding and seriously affect the performance of the seed-metering device [10–14]. Previously, optimization of the structural motion parameters of the cotton seed-metering device was carried out primarily through calculation and test methods, which was time-consuming and labor-intensive. The discrete element method is applicable to the process of cotton seeding as it is a problem of particle fluid motion and complex species interactions. The numerical simulation of the seed-metering process using the discrete element method is helpful to reveal the seed-metering mechanism. It then optimizes the structural and working parameters of seeding. It can also improve development efficiency, improve mechanical performance and reduce costs [15,16].

Accurate calibration will improve DEM results, resulting in the need to determine appropriate material and contact parameters. Therefore, optimizing the discrete element model and parameters of cotton seeds can ensure the accuracy of the prediction of the simulation results [17,18]. In the published research on the calibration of discrete element simulation parameters, most of the calibration objects were corn, rice, wheat, potato, oil sunflower, Panax notoginseng, and other materials, which provide discrete element parameter references for the simulation of related materials [19–26]. Few studies, however, examined the discrete element simulation parameter calibration of cotton seed. Cotton seeds are small in size and irregular in shape, which makes it difficult to determine calibration values by only using actual experiments. To prevent the simulation effect from being distorted, it is important to reasonably determine the discrete element model of cotton seeds and related parameters. So, this study selected cotton seeds as the research object and adopted the method of combining a physical test and simulation test to calibrate the simulation parameters of cotton seeds. Then, the Plackett–Burman test was conducted to determine the significance of the simulation parameters and the steepest climbing test was used to determine the optimal value range of the significant parameters. This test used the response surface analysis method to establish a second-order mathematical model between the significant parameters and each index. The multi-objective optimization calculation was carried out with a NSGA-II algorithm to obtain the optimal solution set with more convergence and diversity. Validation experiments were also conducted. This study provides a reference method for the calibration of the discrete element simulation parameters of cotton seeds and other similar granular materials.

2. Materials and Methods

2.1. Determination of the Intrinsic Parameters of Cotton Seeds

In this study, the cotton variety Xinluzao 78 was selected as the test object. It is widely used in the mechanized production of cotton. This variety has the characteristics of strong boll formation and high yield. Cotton seeds are granular materials, and their intrinsic parameters include external dimensions (length $L \times$ width $W \times$ thickness T), a thousand-seed mass, density, moisture content, Poisson's ratio, elastic modulus, and shear modulus.

2.1.1. Three-Dimensional Geometric Model and Distribution Law

To accurately build a 3D model of cotton seeds, 100 grains were randomly selected in the cotton growing area of Tiemenguan City, Xinjiang, China. Their three-axis dimensions (maximum length L, maximum width W, and maximum thickness T) were measured using ABS origin digital vernier calipers (Matsuzaki brand, accuracy 0.01 mm, range 0–150 mm) [27], as shown in Figure 1. The measurement results were averaged, and the equivalent diameter D and sphericity φ were calculated using Equation (1); the results are shown in Table 1.

$$\begin{cases} D = \sqrt[3]{LWT} \\ \varphi = \frac{D}{L} \times 100\% \end{cases} \tag{1}$$

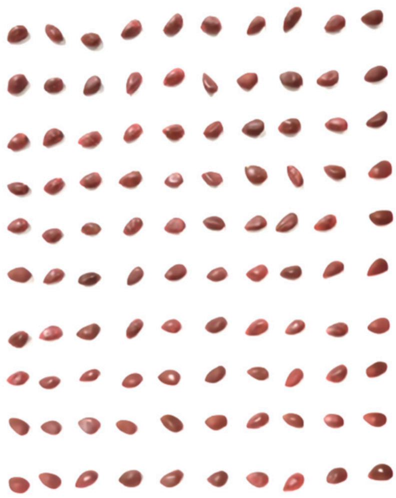

Figure 1. Cotton sample.

Table 1. Determination results of three-axis dimensions of Xinluzao No. 78 cotton seeds.

3D Size	Maximum/mm	Minimum/mm	Average/mm	Standard Deviation	Equivalent Diameter/mm	Sphericity/%
Length	9.67	7.79	8.52	0.43	5.56	65.26
Width	5.38	3.54	4.50	0.32		
Thickness	5.43	3.57	4.48	0.41		

Table 1 shows that the average values of the maximum length L, maximum width W, and maximum thickness T of cotton seeds were 8.52, 4.50, and 4.48 mm, respectively. The standard deviations were 0.43, 0.32, and 0.41, respectively. The equivalent diameter D was 5.56 mm. The sphericity φ was 65.26%, and the cotton seeds were ellipsoid in shape.

2.1.2. Density and Moisture Content

Three separate batches (every batch included 1000 cotton seeds that were randomly selected) were weighed three times using an intelligent electronic balancer (accuracy 0.01 g). The results were averaged to obtain a thousand-grain mass of cotton seeds of 84.40 g. The pycnometer test method was used to measure the volume of 1000 cotton seeds, as shown in Figure 2. A clean pycnometer was filled with distilled water and slowly plugged with a frosted glass stopper. The excess liquid overflowed from the capillary, and the total mass of the pycnometer was recorded as ma; the above 1000 cotton seeds mb were placed into a pycnometer filled with water. The total mass of the pycnometer was recorded as mc, and the mass of the overflowing liquid was recorded as md. It was calculated using Formula (2) that the average volume of 1000 cotton seeds was 129 cm^3. According to these calculations (Mass/Volume), the seed density of Xinluzao No. 78 cotton was 652 kg/m^3. The 1000 cotton seeds were dried in a DHG-9240A electric heating blast drying oven, and after cooling them to room temperature, the dry basis method was used [27]. It was repeated the test 3 times, and the Equation (2) was used to determine the average moisture content of cotton seeds (4.45%):

$$\begin{cases} V = \dfrac{m_d}{\rho} = \dfrac{m_a + m_b - m_c}{\rho} \\ M = \dfrac{m_2}{m_1} \times 100\% \end{cases} \quad (2)$$

where ρ is the density of distilled water, g/cm^3; V is the average volume of 1000 cotton seeds, cm^3; M is the moisture content on the dry basis, %; m_1 is the mass of dry matter contained in the material, g; and m_2 is the mass of moisture contained in the material, g.

Figure 2. Pycnometer.

2.1.3. Poisson's Ratio, Elastic Modulus, and Shear Modulus

Poisson's ratio, also known as the lateral deformation coefficient, reflects the elastic constant of the lateral deformation of the material. A total of 10 cotton seeds were randomly selected from these samples. It was placed horizontally on the bearing plate and the cotton seed was secured in the center of the bearing plate. Using a rigid plate, pressure was applied along the thickness direction of the cotton seeds with a material universal testing machine (loading speed 0.1 mm/s) until the cotton seeds broke (as shown in Figure 3). The deformation amount of the normal strain in the thickness direction (axial) of the cotton seed was read by a material universal testing machine and the average value was 1.19. The deformation of the normal strain in the width direction (transverse direction) was measured with a digital vernier caliper and the average value was 0.26 [28]. The Poisson's ratio of cotton seeds was calculated using Equation (3), and the average value of 10 test results was 0.22.

$$\mu = \frac{|\varepsilon_1|}{|\varepsilon_2|} = \frac{W_1 - W_2}{T_1 - T_2} \quad (3)$$

where μ is the Poisson's ratio of the cotton seeds; ε_1 is the deformation of the cotton seeds in the width direction, mm; ε_2 is the amount of deformation in the thickness direction of the cotton seeds, mm; W_1 is the width of the cotton seeds before loading, mm; W_2 is the width of the cotton seeds after loading, mm; T_1 is the thickness of the cotton seeds before loading, mm; and T_2 is the thickness of the cotton seeds after loading, mm.

The elastic modulus is a scale used to measure the resistance of a material to elastic deformation. During the test, the thickness T_1 was measured before the compression of 10 randomly selected cotton seeds using a digital vernier caliper. It was placed naturally on the circular platform of the material universal testing machine and a circular indenter with a diameter of 5 mm was used, which was perpendicular to the circular platform. Cotton seeds were loaded at a loading speed of 5 mm/min and a loading distance of 3 mm. The universal testing machine was connected to the computer to automatically collect and read the force F-deformation ΔT data. According to the research results of Wang Long et al. [29], the contact area was 0.199 mm^2. This experiment for 10 cotton seeds was repeated. The average value of the elastic modulus calculated from Equation (4) was 2.29 MPa, and the average value of shear modulus was 0.94 MPa. The equation is as follows:

$$\begin{cases} E = \dfrac{F}{\delta A} \\ \delta = \lim\limits_{T_1 \to 0} \dfrac{\Delta T}{T_1} \\ G = \dfrac{E}{2(1+\mu)} \end{cases} \tag{4}$$

where E is the elastic modulus of the cotton seeds, MPa; F is the axial load on the cotton seeds, N; A is the contact area, mm^2; δ is the strain; ΔT is the deformation of the cotton seeds after compression, mm; G is the shear modulus, MPa; and μ is the Poisson's ratio of the cotton seeds.

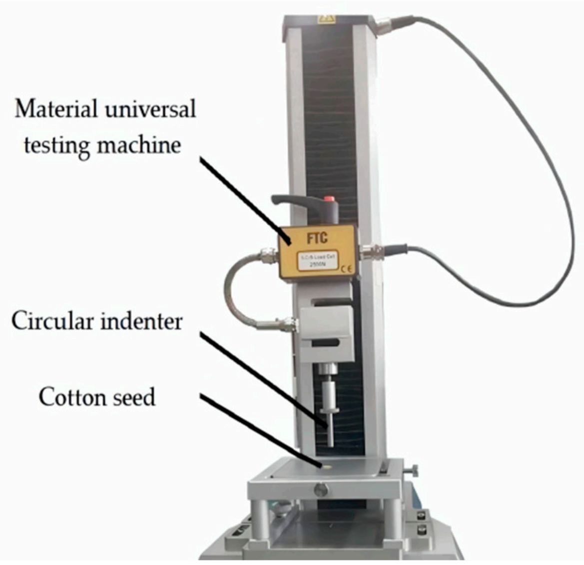

Figure 3. Material universal testing machine.

2.1.4. Establishment of Discrete Element Model of Cotton Seed Based on 3D Scanning

The shape of cotton seeds is an irregular body, and conventional modeling methods cannot accurately restore its actual characteristics. In this study, the cotton seeds whose length, width, and thickness were close to the noted average values (as shown in Figure 4a) were selected as the research objects. Using 3D scanning technology, the outer contour of the cotton seeds were scanned using a PTOP300BS four-eye 3D scanner (measurement point distance 0.02–0.30 mm, automatic splicing) (as shown in Figure 4b). According to the research results of Zhang et al. [30], when building a simulation model, more consideration was given to the particle–particle and particle–material interactions. When performing the parameter calibration, it was necessary to round the corners of the material to ensure authenticity. The cotton seed point cloud data were exported to Geomagic Studio software, and noise points were sharpened to obtain a 3D model of the cotton seeds (as shown in Figure 4c) [25,31,32]. The 3D model of the cotton seeds was imported into the EDEM 2020 software. The smoothing value was set to 2. Using the automatic filling method of the software, a discrete element model of cotton seeds composed of 115 unequal diameter particles was obtained (as shown in Figure 4d) and the minimum particle radius was set to 0.35 mm.

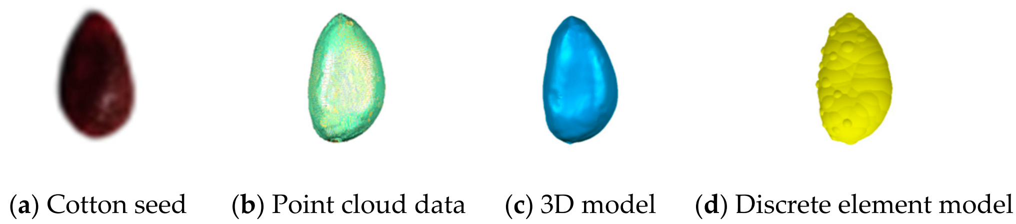

Figure 4. Construction process of cotton seeds discrete element model.

2.2. Exposure Parameter Determination

2.2.1. Contact Model Selection

In addition to particle-to-particle contact, there were also forces with other materials. In this study, materials in contact with cotton seeds included stainless steel and nylon, whose parameters are shown in Table 2 [33,34]. Because there is no adhesion between cotton seeds and the materials in the actual test, the Hertz–Mindlin nonslip contact model was selected for the EDEM simulation. The contact parameters included the coefficients of restitution, static friction, and rolling friction between seeds as well as between seeds and stainless steel and nylon.

Table 2. Simulation parameters of contact materials.

Material	Nature	Value
Cotton seeds	Poisson's ratio	0.22
	Shear modulus/Pa	0.94×10^6
	Density/(kg/m^3)	652.19
Stainless steel	Poisson's ratio	0.3
	Shear modulus/Pa	7×10^{10}
	Density/(kg/m^3)	7800
Nylon	Poisson's ratio	0.4
	Shear modulus/Pa	1×10^8
	Density/(kg/m^3)	1500

2.2.2. Collision Recovery Coefficient Determination

The collision restitution coefficient is an important parameter in particle analysis. This parameter measures the ability of an object to return to its original shape after collision. The freefall collision method (Figure 5a) was used to calibrate the collision restitution coefficient between seeds and between seeds and materials. The test seed population were pasted on a measurement plane using adhesive glue to make a seed plate (Figure 5b). During this test, seeds were released at a height of h = 150 mm from the collision material plate. As soon as the seeds hit the material plate, they rebounded, and the highest rebound height h' was measured by a high-speed camera system. According to Newton's law of collision [35,36], for two objects known to the material, the coefficient of restitution is the ratio of the relative velocity of the two objects separated after collision to the relative approach velocity before collision (that is, the ratio of the highest rebound height h of the collision between the seed and the material and the initial falling height H; because the material does not do the work, the speed before and after the collision is 0). Equation (5) is as follows:

$$e = \left| \frac{v_2{}' - v_1{}'}{v_1 - v_2} \right| == \left| \frac{-\sqrt{2gh'}}{\sqrt{2gh}} \right| = \sqrt{\frac{h'}{h}} \tag{5}$$

where v_1 and v_2 are the velocities of the seeds and materials after the collision, respectively, m/s; and $v_1{}'$ and $v_2{}'$ are the velocities of the seeds and materials before the collision, respectively, in m/s.

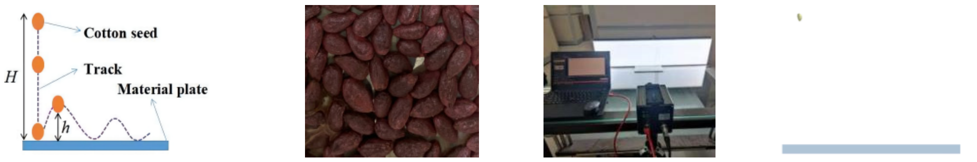

(**a**) Collision principle (**b**) Seed plate (**c**) Actual test (**d**) Simulation test

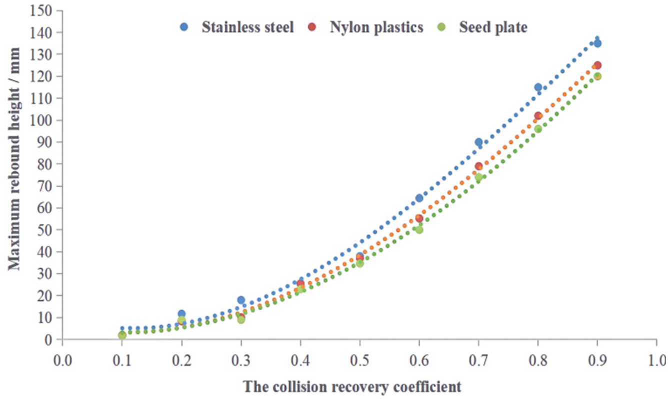

(**e**) Fitting curve of the collision recovery coefficient and maximum rebound height

Figure 5. Collision recovery coefficient determination test and results of the seeds and seed plates, stainless steel, nylon.

A high-speed camera system (including SP-12000C-CXP4 high-speed camera, controller, camera fixed frame, and LED light source) was selected to collect the seed drop video and photos. The seed collision recovery coefficient test system device included a high-speed camera system and a drop frame. The TEMA Starter T2021-003C software data processing module was used to analyze the saved video of the seed falling process, and one point was set as the coordinate reference origin. To determine the restitution coefficient of the seed, the displacement curve of the seed falling and the entire collision process were obtained by using the software tracking function. The test was repeated five times (Figure 5c), the coefficient of restitution was calculated using Equation (5), and the results were averaged. The average maximum rebound heights of the seeds and seed plates, stainless steel, and nylon plastics obtained from the actual test were 19.67, 38.20, and 25.50 mm, respectively, and the coefficients of restitution were 0.36, 0.50, and 0.41.

During the simulation test (Figure 5d), the contact parameters, except the collision restitution coefficient, were set to 0. Taking the coefficient of restitution e as the factor and the highest rebound height h as the index, the range of the coefficient of restitution of the collision between cotton seeds and the contact material was 0.1–0.9, and the interval was 0.1. Each group of tests was repeated five times to obtain the mean value. The test results were drawn in a scatter diagram and fitted to the curve (Figure 5e), and the following fitting equation was obtained:

$$\begin{cases} h_1 = -124.92e_1^3 + 357.43e_1^2 - 78.18e_1 + 9.5216 \\ \quad\quad (R^2 = 0.9942) \\ h_2 = -79.887e_2^3 + 282.2e_2^2 - 56.069e_2 + 5.9966 \\ \quad\quad (R^2 = 0.9983) \\ h_3 = -35.844e_3^3 + 221.1e_3^2 - 41.494e_3 + 5.1787 \\ \quad\quad (R^2 = 0.9977) \end{cases} \quad (6)$$

where h_1, h_2, and h_3 are the maximum rebound heights of seeds and seed plates, stainless steel, and nylon, respectively, in mm; e_1, e_2, and e_3 are the collision recovery coefficients of seeds and seed plates, stainless steel, and nylon, respectively.

There was a positive correlation between the collision recovery coefficient and the maximum rebound height, and the coefficients of determination of the equations R^2 were all greater than 0.99. Therefore, it could be used to calibrate the collision recovery coefficient between seeds and seed plates, stainless steel and nylon. Substituting the mean maximum rebound heights of 19.67, 38.40, and 25.50 mm of the seeds and seed plates, stainless steel, and nylon obtained from the actual test into Equation (6), the collision recovery coefficients for e were 0.38, 0.47, and 0.41, respectively. These values were substituted into the EDEM simulation verification, and the relative errors (the relative error could better reflect the reliability of the measurement, which is the relative error = | simulation value − physical value | /physical value) of the measured collision recovery coefficients were 5.56%, 6.0%, and 0.0%, respectively, which met the reasonable error range. Therefore, the collision recovery coefficients for e of the seeds and seed plates, stainless steel, and nylon were set as 0.38, 0.47, and 0.41, respectively.

2.2.3. Static Friction Factor Determination

The coefficient of static friction is the ratio of the maximum static friction force experienced by the material to the normal positive pressure, which can be used to express the friction properties between the material and the solid surface in contact [37]. In this study, the incline method was used to measure the static friction coefficient between cotton seeds, and between cotton seeds and stainless steel and nylon. A digital display inclinometer (with an accuracy of 0.05°) was used to measure the inclination angle during the test (Figure 6a). To prevent seeds from rolling, four seeds were glued together and placed directly on the measuring plane. The seeds slowly turned the inclinometer test plane counterclockwise. When the cotton seeds began to slide, the inclination angles between the cotton seeds and the seed plate, the stainless steel, and the nylon were recorded as 23.03°, 29.18°, and 34.7°, respectively. Five repeated experiments were performed to obtain the average α. Using Equation (7), the static friction coefficients between cotton seeds and seed plates, stainless steel, and nylon were calculated, and the average values obtained were 0.43, 0.56, and 0.69, respectively. Equation (7) is as follows:

$$\mu = \frac{f}{F} = \frac{mg\sin\alpha}{mg\cos\alpha} = \tan\alpha \tag{7}$$

During the simulation, the static friction coefficient μ between the seed and the seed plate, stainless steel, and nylon were used as the factor. The angle α between the inclined plane and the horizontal plane as the index was used to conduct the test in the EDEM (using the calibrated collision recovery coefficient). Other contact parameters were set to 0, the static friction factor range was selected from 0.1 to 0.9, and the test horizontal interval was 0.1 (Figure 6b). To avoid the seeds from rolling on the slope, four bonded pellet replacement models were placed at one end of the slope. The same parameters were set as the actual test for the simulation, and when the seeds started to slide, the inclined angle α between the inclined plane and the horizontal plane was recorded. The test was repeated five times, and the results were averaged. The test results were plotted into a scatter plot and fit the curve (Figure 6c). Then, the equation was fit to obtain the following:

$$\begin{cases} \alpha_1 = -13.485\mu_1^3 + 20.987\mu_1^2 + 34.948\mu_1 + 3.3343 \\ \qquad (R^2 = 0.9980) \\ \alpha_2 = 3.3838\mu_2^3 - 11.745\mu_2^2 + 53.777\mu_2 + 1.2224 \\ \qquad (R^2 = 0.9966) \\ \alpha_3 = -4.3939\mu_3^3 + 3.3117e_3^2 + 46.332e_3 + 2.7271 \\ \qquad (R^2 = 0.9977) \end{cases} \tag{8}$$

where α_1, α_2, and α_3 are the angles between the inclined plane and the horizontal plane between the seed and the seed plate, the stainless steel, and the nylon plastic, respectively, in degrees; and μ_1, μ_2, and μ_3 are the static friction coefficients of the seeds and seed plates, stainless steel, and nylon plastics, respectively.

(**a**) Actual test

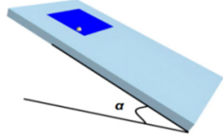

(**b**) Simulation test

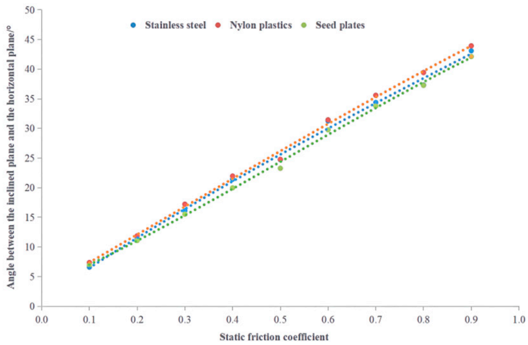

(**c**) Fitting curve of the static friction coefficient and angle between the inclined plane and the horizontal plane

Figure 6. Static friction factor determination test and results of the seeds and seed plates, stainless steel, nylon.

There was a positive correlation between the static friction coefficient and angle, and the coefficients of determination of the equations R^2 were all greater than 0.99. Therefore, they could be used to calibrate the static friction factor between seeds and seed plates, stainless steel and nylon. Substituting the included angles measured in the actual test into Equation (8), respectively, the μ between the cotton seed and the seed plate, stainless steel, and nylon was 0.47, 0.58, and 0.69, respectively. These values were substituted into EDEM to verify that the relative errors of the measured static friction coefficient were 9.30%, 3.60% and 0.0%, respectively, which met the reasonable error range. Therefore, the μ between the cotton seed and the seed plate, stainless steel, and nylon was set as 0.47, 0.58, and 0.69, respectively.

2.2.4. Determination of Rolling Friction Factor

Rolling friction refers to the resistance to rolling caused by the deformation of two objects in the contact part when one object rolls without slip or has a tendency to roll on the surface of another object [25]. The rolling friction factor was determined the same way as the static friction factor, that is, using the inclined surface rolling method. Because of the rolling friction, the seeds eventually rolled down onto the horizontal panel and came to rest. Assuming that the seed is an ideal sphere, it is affected only by rolling friction during the pure rolling process. Then, the rolling friction force can be obtained according to the law of the conservation of energy, as follows:

$$\begin{cases} mgS\sin\beta = mg(S\cos\beta + L)\mu_s \\ \mu_s = \dfrac{S\sin\beta}{S\cos\beta + L} \end{cases} \tag{9}$$

where β is the inclination angle, in degrees; S is the rolling distance along the inclined plane, in mm; and L is the horizontal scrolling distance, in mm.

Because cotton seeds are not ideal spheres, to ensure the accuracy of the test results, it was necessary to select an appropriate inclination angle and inclined plane rolling distance. Referring to the research results of Zhang Shengwei et al. [38], the inclination angle was set to 45° and the rolling distance of the inclined plane was set to 30 mm. The seeds were released at an initial speed of 0, so that the seeds could roll down the slope. When the seeds were stationary, the horizontal rolling distance of the seeds was measured (Figure 7a). To further reduce the experimental error, the average value of five repeated experiments were taken. The test results showed that the horizontal rolling distances between the seeds and the seed plate, stainless steel, and nylon were 74, 101, and 132 mm, respectively. By substitution into Equation (9), the corresponding rolling friction coefficients were 0.15, 0.12, and 0.09, respectively. The simulation test adopted the same method, and the calibrated collision restitution coefficient and static friction coefficient were set in EDEM (Figure 7b). Other contact parameters were set to 0, taking the rolling friction factor as a factor. The factor range was selected from 0.08 to 0.16, and the test level interval was 0.01. Taking the horizontal scrolling distance as the evaluation index, the test results were drawn into a scatter diagram and fitted to the curve (Figure 7c). Then, the following fitting equation was obtained:

$$\begin{cases} L_1 = -62290{\mu_{s}}_1^3 + 29697{\mu_{s}}_1^2 - 5452.9\mu_{s_1} + 425.16 \\ \quad (R^2 = 0.9977) \\ L_2 = -5050.5{\mu_{s}}_2^3 + 9080.1{\mu_{s}}_2^2 - 3006.7\mu_{s_2} + 334.5 \\ \quad (R^2 = 0.9986) \\ L_3 = -50505{\mu_{s}}_3^3 + 25162{\mu_{s}}_3^2 - 4855.9\mu_{s_3} + 400.99 \\ \quad (R^2 = 0.9977) \end{cases} \tag{10}$$

where L_1, L_2, and L_3 are the horizontal rolling distances of seeds on the seed plate, stainless steel, and nylon plastic, respectively, in mm; μ_{s1}, μ_{s2}, and μ_{s3} are the rolling friction coefficients of the seed and seed plate, stainless steel, and nylon plastic, respectively.

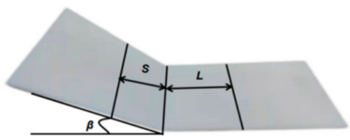

(**a**) Actual test

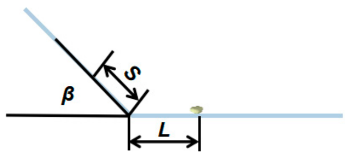

(**b**) Simulation test

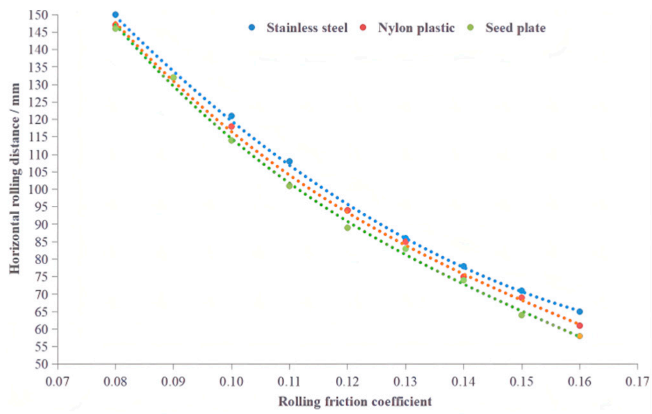

(**c**) Fitting curve of the rolling friction coefficient and horizontal rolling distance

Figure 7. Rolling friction factor determination test and results of the seeds and seed plates, stainless steel, nylon.

There was a positive correlation between the rolling friction coefficient and horizontal rolling distance, and the coefficients of determination of the equations R^2 were all greater than 0.99. Therefore, it could be used to calibrate the rolling friction factor between seeds and seed plates, stainless steel and nylon. The average value of the horizontal rolling distance between the actually measured seeds and the seed plate, stainless steel, and nylon were substituted into Equation (10) to obtain the corresponding seed rolling friction factors of 0.14, 0.12, and 0.08, respectively. These values were substituted into EDEM to verify that the relative errors of the measured rolling friction coefficient were 6.67%, 0.0%, and 11.1%, respectively, which met the reasonable error range. Therefore, the rolling friction factors between the seed and seed plate, stainless steel, and nylon were taken as 0.14, 0.12, and 0.08, respectively.

3. Results and Discussion

3.1. Stacking Angle and Angle-of-Repose Test

Various complex motion states in the process of forming the accumulation angle of the bulk material can better characterize the scattering, flow, and friction characteristics of the bulk material [27]. The stacking angle and angle of repose are important basic data for material transportation, storage, harvesting, sowing, and other links [27,39,40]. Referring to the research results of Liu et al. [19,38], a self-made container was selected (300 mm in length, 150 mm in width, and 310 mm in height). A partition was arranged in the middle. When measuring, the inoculation disc was placed directly below the seed drop opening. The seeds were poured from the top of the container and a horizontal scraper was used to remove the excess seeds on the top of the container. The seeds kept flush with the top surface of the container. The movable plate was slowly pulled out from the middle of the partition, and the seeds went through seeding, accumulation, and stillness. Then, a stable angle of repose formed on both sides of the area above the container, and a stable angle of accumulation formed at the inoculation disc. The material of the device was transparent resin. When all of the cotton seeds were stationary and the slope was stable, a camera was used to take vertical pictures of the front and both sides of the pile, as shown in Figure 8.

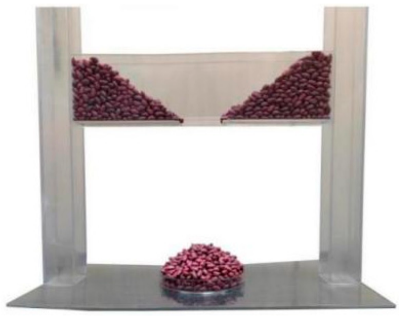

Figure 8. Determination test of stacking angle and angle-of-repose.

To further reduce the manual measurement error, Matlab (Full name: Matrix Laboratory) software was used to process the stacking angle image obtained from the experiment [41]. The specific processing method was as follows: First, the original image was performed grayscale processing (Figure 9a). Second, an appropriate threshold was selected for binarization and the bwperim function was used to extract the contour of the binary image (Figure 9b). Because the bwperim function extracted the outer contour, it also extracted the inner edge enclosed by the holes inside the graphics area. Third, the imfill function was used to fill and dilate the inner edge to obtain a complete edge contour (Figure 9c). Fourth, the edge contours were transformed into coordinate data and linear fitting was performed using the image digitizing tool (Figure 9d). Fifth, the slope obtained with linear fitting was converted into an angle, which was the stacking angle and the angle of repose of the cotton seed physical stacking test. This test was repeated 10 times, and the average value was obtained. The accumulation angle and angle of repose of the cotton seed physical accumulation test were 29.09° and 34.88°, respectively.

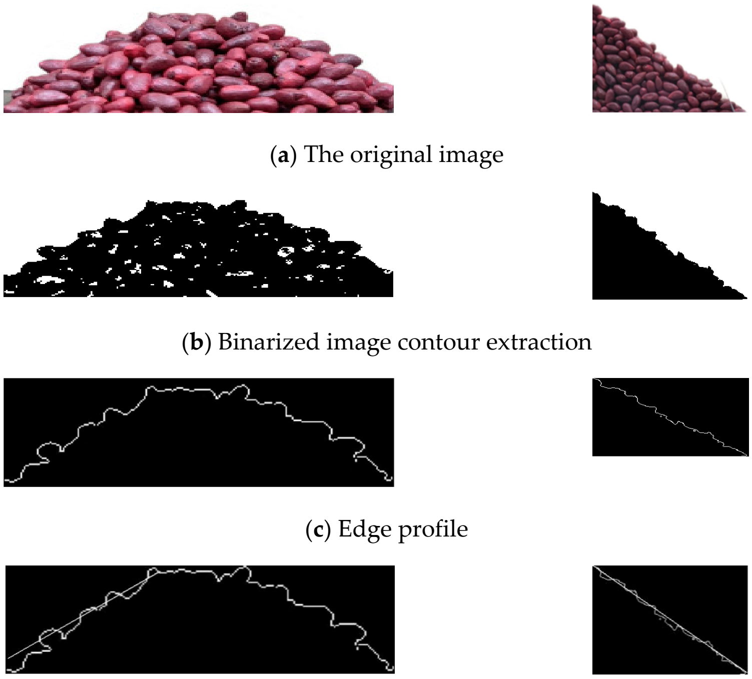

(**a**) The original image

(**b**) Binarized image contour extraction

(**c**) Edge profile

(**d**) Fitting line

Figure 9. Edge contour extraction process of stacking angle and angle of repose.

3.2. Determining Significant Influence Parameters

The Plackett–Burman experimental design was carried out with Design-Expert software, and the selection of experimental parameters was based on the results of physical tests. Taking the stacking angle and angle of repose of cotton seeds as the response values, the parameters that had a significant effect on the response value were screened out using the Plackett–Burman test [22]. The maximum and minimum values of the eight test parameters in Table 3 were coded as levels +1 and −1, respectively. The Plackett–Burman test scheme and results are given in Table 4. After each set of simulation tests, the stacking angle and angle of repose of the cotton seed pile were measured, as shown in Figure 10. The Design-Expert 12.0 software was used to perform the variance analysis on the test results and the significance results of each simulation parameter was obtained, as shown in Table 5. X_1, X_2, X_3, X_4, X_8, X_9 and X_{10} had little effect on the stacking angle and angle of repose, and the contribution rate was less than 5%. The contribution rate of X_5, X_6 and X_7 to the stacking angle and the angle of repose was relatively high, which had a significant influence on their formation.

Table 3. Plackett–Burman test parameter range table.

Test Parameters	Low Level	High Level
Cotton seed-steel plate collision recovery coefficient X_1	0.2	0.4
Cotton seed-steel plate static friction coefficient X_2	0.3	0.5
Cotton seed-steel plate rolling friction coefficient X_3	0.1	0.3
Cotton Seed Poisson's Ratio X_4	0.1	0.3
Cotton Seed—Cotton Seed Recovery Factor X_5	0.3	0.5
Cotton Seed—Cotton Seed Static Friction Coefficient X_6	0.4	0.6
Cotton Seed—Cotton Seed Rolling Friction Coefficient X_7	0.1	0.3
Cotton Seed-Nylon Plastic Collision Recovery Coefficient X_8	0.5	0.7
Cotton Seed-Nylon Plastic Coefficient of Static Friction X_9	0.6	0.8
Cotton Seed-Nylon Plastic Coefficient of Rolling Friction X_{10}	0.1	0.3
X_{11}, X_{12}, X_{13}, X_{14}	Dummy parameter	

Table 4. Plackett–Burman test protocol and results.

No.	Test Parameters											Stacking Angle/°	Angle of Repose/°
	X_1/X_8	X_2/X_9	X_3/X_{10}	X_4	X_5	X_6	X_7	X_{11}	X_{12}	X_{13}	X_{14}		
1	−1	1	1	1	−1	−1	−1	1	−1	1	1	34.78/36.48	38.24/40.20
2	−1	1	−1	1	1	−1	1	1	1	−1	−1	38.96/40.10	43.78/45.90
3	−1	1	1	−1	1	1	1	−1	−1	−1	1	43.64/45.78	47.70/50.10
4	1	1	−1	1	1	1	−1	−1	−1	1	−1	39.13/41.12	43.19/45.39
5	1	−1	−1	−1	1	−1	1	1	−1	1	1	40.78/42.82	45.56/47.90
6	−1	−1	−1	1	−1	1	1	−1	1	1	1	39.10/40.09	41.91/44.08
7	−1	−1	−1	−1	−1	−1	−1	−1	−1	−1	−1	35.46/36.89	38.63/40.06
8	1	1	−1	−1	−1	1	−1	1	1	−1	1	36.88/39.01	41.20/44.30
9	−1	−1	1	−1	1	1	−1	1	1	1	−1	39.50/41.37	42.80/44.84
10	1	−1	1	1	−1	1	1	1	−1	−1	−1	39.55/40.53	42.51/44.70
11	1	−1	1	1	1	−1	−1	−1	1	−1	1	35.58/38.36	40.50/42.59
12	1	1	1	−1	−1	−1	1	−1	1	1	−1	35.11/37.02	38.76/40.10

Figure 10. Simulation test of accumulation angle and angle of repose.

3.3. Steepest Climb Test

On the basis of the Plackett–Burman test, X_5, X_6 and X_7 were selected, which had a larger contribution rate and a more significant impact on the stacking angle and angle of repose. In the subsequent climbing test and response surface optimization test, optimization was carried out and the remaining parameters from the values obtained previously were selected. Taking X_5, X_6 and X_7 as the test factors, the steepest climbing test was carried out. The accumulation-angle error Y_1 and the angle-of-repose error Y_2 of the steepest climbing test were calculated from Equation (11) and used as the test index. The design and results of the steepest climbing test are shown in Table 6. Table 6 shows that with an increase in X_5, X_6 and X_7, the accumulation-angle error Y_1 and the angle-of-repose error Y_2 of the steepest climbing test followed a trend of decreasing first and then increasing, and the relative error was the smallest under the parameters of Experiment 3. Therefore, the parameters of Experiment 3 were selected as the intermediate level, and the parameters of Experiment 2 and Experiment 4 were selected as the low level and the high level, respectively, for the subsequent response surface optimization experiments. The value ranges of the collision recovery coefficient, static friction coefficient, and dynamic friction coefficient between cotton seeds were 0.35–0.45, 0.65–0.75, and 0.15–0.25, respectively. Thus, the following was obtained:

$$\begin{cases} Y_1 = \dfrac{\alpha - \alpha_1}{\alpha_1} \\ Y_2 = \dfrac{\beta - \beta_1}{\beta_1} \end{cases} \tag{11}$$

where α is the actual test value of the stacking angle, in degrees; α_1 is the simulation test value of stacking angle, in degrees; β is the actual test value of the stacking angle, in degrees; and β_1 is the simulation test value of stacking angle, in degrees.

Table 5. Significance analysis of Plackett–Burman test parameters.

Parameter	Angle of Repose Error				Stacking Angle Error			
	Normalization Effect	Sum of Square	Contribution Rate	Significance Ranking	Normalization Effect	Sum of Square	Contribution Rate	Significance Ranking
X_1/X_8	−0.735/ −0.308333	1.62067/ 0.285208	2.04183/ 0.359257	4/ 5	−0.22333/ −0.0333333	0.149633/ 0.00333333	0.167211/ 0.00314385	6/ 7
X_2/X_9	−0.245/ 0.0916667	0.180075/ 0.0252083	0.22687/ 0.0317532	7/ 6	0.16/ 0.303333	0.0768/ 0.276033	0.0858219/ 0.260342	7/ 6
X_3/X_{10}	−0.358333/ −0.081667	0.385208/ 0.0200083	0.485311/ 0.0252031	6/ 7	−0.626667/ −0.85	1.17813/ 2.1675	1.31653/ 2.04429	5/ 4
X_4	−0.711667/ −1.035	1.51941/ 3.21367	1.91425/ 4.04805	5/ 4	−0.753333/ −0.74	1.70253/ 1.6428	1.90253/ 1.54942	4/ 5
X_5	2.785/ 3.255	23.2687/ 31.7851	29.3154/ 40.0375	2/ 1	3.71333/ 3.88	41.3665/ 45.1632	46.2259/ 42.5959	1/ 1
X_6	2.855/ 2.705	24.4531/ 21.9511	30.8076/ 27.6503	1/ 2	2.30667/ 2.77667	15.9621/ 23.1296	17.837/ 21.8149	3/ 2
X_7	2.635/ 2.185	20.8297/ 14.3227	26.2426/ 18.0413	3/ 3	2.61/ 2.56667	20.4363/ 19.7633	22.837/ 18.6399	2/ 3

Table 6. Steepest incline test plan and results.

No.	X_5	X_6	X_7	Y_1	Y_2
1	0.30	0.60	0.10	26.49	24.03
2	0.35	0.65	0.15	10.70	8.84
3	0.40	0.70	0.20	4.22	2.62
4	0.45	0.75	0.25	13.33	9.81
5	0.50	0.80	0.30	24.92	28.85

3.4. Response Surface Optimization Test and Regression Model Establishment

To further obtain the optimal contact parameter combination, the interspecies collision restitution coefficient, interspecies static friction factor, and interspecies rolling friction factor were used as test factors. By applying the stacking-angle error and angle-of-repose error as test indicators, a three-factor quadratic rotation orthogonal combination simulation test was carried out. The test factor codes are given in Table 7, and the test plan and test results are provided in Table 8. Each group of experiments was repeated three times to obtain the average value.

Table 7. Response surface optimization test of factors and levels.

Level	Interspecies Collision Coefficient of Restitution X_5	Interspecies Static Friction Factor X_6	Interspecies Rolling Friction Factor X_7
−1.682	0.32	0.62	0.12
−1	0.35	0.65	0.15
0	0.40	0.70	0.20
1	0.45	0.75	0.25
1.682	0.48	0.78	0.28

3.5. Test Results and Discussion

3.5.1. Mathematical Model Establishment and Significance Test

Through the multiple regression fitting analysis of the test data in Table 8, the regression model of the influence of each factor on the stacking-angle error and the angle-of-repose error were obtained to further accurately reflect the relationship between each significant factor and the test index, and carry out the predictive analysis of the target value, as shown in Equation (12). It can also be used for the prediction analysis of the target value. The analysis of variance was performed, as shown in Table 9.

Table 8. Response surface optimization test of protocol and results.

No.	Interspecies Collision Coefficient of Restitution X_5	Interspecies Static Friction Factor X_6	Interspecies Rolling Friction Factor X_7	Stacking Angle Error Y_1/%	Angle of Repose Error Y_2/%
1	0.000	−1.682	0.000	8.03	4.05
2	−1.000	−1.000	−1.000	7.39	7.41
3	0.000	0.000	0.000	1.86	2.17
4	0.000	0.000	−1.682	7.08	7.58
5	0.000	0.000	0.000	1.41	2.72
6	1.000	1.000	−1.000	8.42	7.23
7	0.000	1.682	0.000	7.71	6.95
8	−1.000	1.000	1.000	5.32	8.27
9	1.000	−1.000	1.000	4.7	2.7
10	1.000	−1.000	−1.000	7.57	4.06
11	−1.682	0.000	0.000	3.23	8.95
12	0.000	0.000	0.000	1.36	2.02
13	0.000	0.000	0.000	1.76	1.91
14	0.000	0.000	0.000	1.53	2.35
15	−1.000	1.000	−1.000	4.58	7.93
16	0.000	0.000	1.682	4.85	4.63
17	1.000	1.000	1.000	5.43	6.31
18	0.000	0.000	0.000	1.52	2.9
19	−1.000	−1.000	1.000	6.5	6.57
20	1.682	0.000	0.000	3.42	4.04

$$\begin{cases} Y_1 = 1.57 + 0.2013x_5 - 0.2086x_6 - 0.7074x_7 \\ +0.6837x_5x_6 - 0.7263x_5x_7 + 0.1763x_6x_7 \\ +0.6731{x_5}^2 + 2.28{x_6}^2 + 1.61{x_7}^2 \\ Y_2 = 2.34 - 1.33x_5 + 1.02x_6 - 0.5668x_7 \\ +0.57x_5x_6 - 0.2225x_5x_7 + 0.2025x_6x_7 \\ +1.48{x_5}^2 + 1.13{x_6}^2 + 1.34{x_7}^2 \end{cases} \tag{12}$$

Table 9. Variance analysis of stacking angle error and angle of repose error.

Source	Stacking Angle Error				Angle of Repose Error			
	Sum of Square	Degree of Freedom	F	p	Sum of Square	Degree of Freedom	F	p
Model	120.34	9	122.98	<0.0001	109.30	9	55.78	<0.0001
x_5	0.5536	1	5.09	0.0477	24.09	1	110.65	<0.0001
x_6	0.5940	1	5.46	0.0415	14.10	1	64.77	<0.0001
x_7	6.83	1	62.85	<0.0001	4.39	1	20.16	0.0012
x_5x_6	3.74	1	34.40	0.0002	2.60	1	11.94	0.0062
x_5x_7	4.22	1	38.81	<0.0001	0.3960	1	1.82	0.2072
x_6x_7	0.2485	1	2.29	0.1615	0.3280	1	1.51	0.2477
${x_5}^2$	6.53	1	60.04	<0.0001	31.50	1	144.69	<0.0001
${x_6}^2$	74.91	1	688.99	<0.0001	18.29	1	84.02	<0.0001
${x_7}^2$	37.19	1	342.05	<0.0001	25.90	1	118.96	<0.0001
Residual	1.09	10			2.18	10		
Lack of fit	0.8934	5	4.61	0.0595	1.40	5	1.81	0.2649
Pure error	0.1939	5			0.7742	5		
Total	121.43	19			114.48	19		

Note: $p < 0.01$ means highly significant, $p < 0.05$ means significant.

According to the variance analysis in Table 9, the p values of the stacking-angle error model and the angle-of-repose error model were both less than 0.0001, which indicated that the regression model was highly significant. The lack-of-fit item p values were 0.0595 and 0.2649, which indicated that the regression model had a high degree of fitting. The coefficients of determination R^2 were 0.9910 and 0.9805, indicating that the model explained more than 99.10% and 98.05% of the evaluation indicators, respectively. Therefore, the regression model was extremely significant, the lack of fit was not significant, and the coefficient of determination was close to 1, which indicated that the regression equation fit well. When using Design-Expert software for the center composite test, a model with an accuracy greater than four has better predictability [42]. The accuracies of the model were 29.1619 and 19.4442, respectively, which indicated that the model could predict the stacking angle and angle of repose of cotton seeds well. The stacking-angle error model has six regression terms x_7, x_5x_6, x_5x_7, $x_5{}^2$, $x_6{}^2$, and $x_7{}^2$, which had extremely significant effects on the regression model ($p < 0.01$). Two regression items (x_5 and x_6) had significant effects on the regression model ($p < 0.05$). One regression item (x_6x_7) did not have a significant effect on the regression model ($p > 0.05$). The angle-of-repose error model had seven regression terms (x_5, x_6, x_7, x_5x_6, $x_5{}^2$, $x_6{}^2$, and $x_7{}^2$), which had a very significant impact on the regression model ($p < 0.01$). Two regression items (x_5x_7 and x_6x_7) did not have a significant effect on the regression model ($p > 0.05$). The optimized equation after removing insignificant regression terms is shown in Equation (13):

$$\begin{cases} Y_1 = 1.57 + 0.2013x_5 - 0.2086x_6 - 0.7074x_7 \\ +0.6837x_5x_6 - 0.7263x_5x_7 + 0.6731x_5{}^2 + 2.28x_6{}^2 + 1.61x_7{}^2 \\ Y_2 = 2.34 - 1.33x_5 + 1.02x_6 - 0.5668x_7 \\ +0.57x_5x_6 + 1.48x_5{}^2 + 1.13x_6{}^2 + 1.34x_7{}^2 \end{cases} \tag{13}$$

3.5.2. Influence of Various Factors on Test Index and Parameter Optimization

According to the analysis results of the regression model, the response surface diagram was drawn with the Design-Expert software. The effects of the interspecies collision recovery coefficient, interspecies static friction factor, and interspecies rolling friction factor on the stacking-angle error and the angle-of-repose error were obtained. The response surface is shown in the Figure 11.

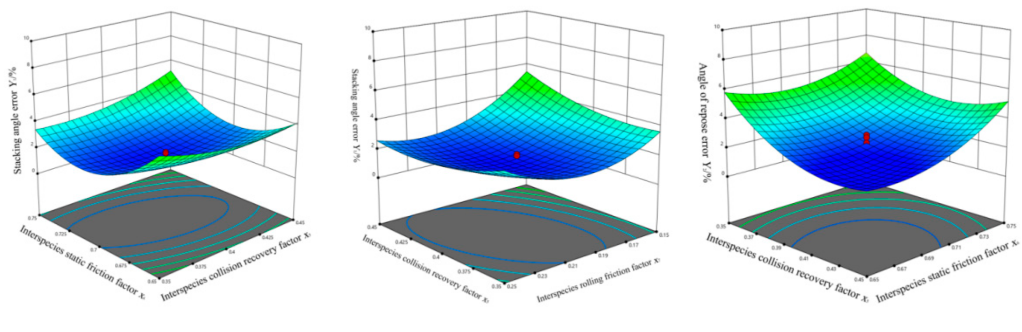

Y_1=（X_5，X_6，0）　　Y_1=（X_5，0，X_7）　　Y_2=（X_5，X_6，0）

Figure 11. Influence of each factor on interaction of the angle-of-repose error and the accumulation-angle error.

To obtain the optimal working parameters of each factor, the parameters of the established ternary quadratic orthogonal regression test were optimized using the Design-Expert data analysis software. In this study, the NSGA-II optimization algorithm was adopted. The unique elite retention strategy and diversity maintenance mechanism of this algorithm ensured the convergence and diversity of its calculation results [43]. Taking the minimum angle-of-repose error and the minimum stacking-angle error as the optimization objectives, the interspecies collision recovery coefficient, the interspecies static friction factor, and the interspecies rolling friction factor were used as the optimization objects of study. On the basis of the previous tests, it was determined that the restitution coefficient of interspecies collision was 0.32–0.48, the interspecies static friction factor was 0.62–0.78, and the interspecies rolling friction factor was 0.12–0.28. Therefore, the objective function and constraint function of the optimization problem are as follows:

$$\begin{cases} \min & Y_1 \\ \min & Y_2 \\ s.t. & 0.32 \leq x_5 \leq 0.48 \\ & 0.62 \leq x_6 \leq 0.78 \\ & 0.12 \leq x_7 \leq 0.28 \end{cases} \quad (14)$$

For multi-objective optimization problems, it is impossible to optimize each objective at the same time. However, coordination and trade-offs could be made between objectives to satisfy each objective to the degree possible. As a result, all solutions on the optimal frontier could be used for scheme optimization. Under the principle of taking into account the angle-of-repose error and the accumulation-angle error, the restitution coefficient of interspecies collision was selected as 0.413, the interspecies static friction factor was 0.695, and the interspecies rolling friction factor was 0.214.

3.6. Verification Test

To verify the accuracy of the optimization results, the optimal combination of simulation parameters for cotton seeds were calibrated using the optimization results and were as follows: the interspecies collision recovery coefficient was 0.413, the interspecies static friction coefficient was 0.695, and the interspecies rolling friction coefficient was 0.214. The values of other non-significant simulation parameters are the same as the mean values of measured data in physical experiments. Taking the previously determined parameters as the EDEM simulation parameters, three repeated simulation experiments were conducted. The relative error between the average value of the physical test accumulation angle of 29.09° and the average value of the simulation test accumulation angle of 29.82° was only 2.50%. Additionally, the relative error of the average value of the physical test angle of repose of 34.88° and the average value of the simulation test angle of repose of 35.28° was only 1.15% (the relative error could better reflect the reliability of the measurement, which was the relative error = |simulation value − physical value|/physical value). The smaller the relative error, the higher the reliability of the measurement results. Thus, the reliability and authenticity of the simulation test were further verified. The results are shown in Table 10.

Table 10. Experiment verification results.

Test No.	Stacking Angle/°	Angle of Repose/°
1	30.01	35.02
2	29.56	35.55
3	29.89	35.26
Average	29.82	35.28
Relative error	2.50	1.15

4. Conclusions

The basic physical parameters of cotton seeds were obtained with a physical test. Based on the freefall collision method, the inclined plane sliding method, and the inclined plane rolling method, the contact values of the coefficients between the cotton seeds and cotton seeds, stainless steel plates, and nylon plastics were measured, respectively. A Plackett–Burman test was used to screen out the significant parameters affecting the accumulation angle and the angle of repose, including the interspecies restitution coefficient, interspecies static friction coefficient, and interspecies rolling friction coefficient. Further, through the steepest climbing test, the optimal ranges of the significant parameters were determined.

Using the Box–Behnken test, the NSGA-II optimization algorithm was adopted to take the minimum error of the angle of repose and the minimum stacking-angle error as the optimization objective and the best simulation was obtained. The best combination of simulation parameters was as follows: a restitution coefficient of interspecies collision of 0.413, interspecies static friction coefficient of 0.695, and interspecies rolling friction coefficient of 0.214. To verify the accuracy of the optimization results, three repeatable simulation experiments were conducted. The relative error of the average accumulation angle of the physical test of 29.09° and the average of the accumulation angle of the simulation test of 29.82° was only 2.50%. The relative error of the mean angle of repose of 35.28° was only 1.15%. The above test results demonstrated that the calibration results were accurate and reliable, which could provide a reference for the simulation of cotton precision seeding operations.

Due to the limitation of computing time and computer performance, in-depth research on the microscopic parameters of material properties should be continued in the future to compensate for the deviation caused by the difference in the shape of granular materials. Moreover, various characteristics of agricultural materials are often closely related to moisture content, and it is necessary to further clarify the influence of different moisture contents on the accumulation angle and angle of repose of cotton seeds. Therefore, the characteristic parameters of cotton seeds under different moisture contents were determined to further improve the accuracy of the model. In the follow-up study, a systematic investigation will be carried out on cotton seeds with different particle sizes and shapes, and the model parameters will be revised, in order to improve the versatility of simulation methods, the accuracy of simulation results and the efficiency of model calculation.

Author Contributions: Conceptualization, Y.Y. and B.Z.; methodology, S.B. and K.N.; software, S.B. and Z.S.; validation, S.B. and Y.Z.; formal analysis, K.N. and S.B.; investigation, G.X. and Y.M.; resources, Y.Y. and B.Z.; data curation, S.B. and L.W.; writing—original draft preparation, S.B.; writing—review and editing, K.N. and L.L.; visualization, S.X. and L.Z.; supervision, Y.Y. and B.Z.; project administration, Y.Y. and K.N.; funding acquisition, K.N. and L.Z. All authors have read and agreed to the published version of the manuscript.

Funding: This work was mainly supported by the Autonomous Region Regional Collaborative Innovation Special (Science and Technology Aid to Xinjiang Program) Project of China (2021E02055).

Data Availability Statement: Data are contained within the article. The data presented in this study can be requested from the authors.

Conflicts of Interest: The authors declare no conflict of interest.

References

1. Wang, S.L. *Research on the Mechanism and Computer Simulation of the Mechanism of the Mechanical Clamp Type Cotton Precision Metering Device*; Shihezi University: Shihezi, China, 2009; (In Chinese with English Abstract)
2. Mao, S.C.; Li, Y.B.; Dong, H.Z.; Bie, S.; Lin, Y.Z.; Dong, H. *Chinese Cotton Cultivation*; Shanghai Scientific & Technical Publishers: Shanghai, China, 2013; (In Chinese with English Abstract)
3. National Bureau of Statistics of People's Republic of China. *China Statistical Yearbook*; China Statistics Press: Beijing, China, 2019; (In Chinese with English Abstract)
4. Liu, L.H.; Yang, R.B.; Shang, S.Q.; Lian, Z.G.; Cui, G.P.; Yang, H.G.; Xu, P.X. Design and Experiment of 2MBJ-2 Subsoiling Tillage Fertilizer Coated Cotton Planter. *J. Agric. Mech. Res.* **2017**, *4*, 134–138. (In Chinese with English Abstract)
5. Liu, L.H. *Design and Experiment Research of High Density Compound Cotton Planter*; Qingdao Agricultural University: Qingdao, China, 2017; (In Chinese with English Abstract)
6. Kang, S.W.; Ni, X.D.; Qi, Q.Z.; Han, S.M. Design and experiment of a suction drum type cotton precision seed metering device. *J. Agric. Mech. Res.* **2020**, *6*, 136–141. (In Chinese with English Abstract)
7. Liu, H.X.; Wang, F.L.; Yang, G.L. Study on a new type vertical composite disc soybean precision seed metering device. *Trans. Chin. Soc. Agric. Eng.* **2007**, *10*, 112–116. (In Chinese with English Abstract)
8. Liu, H.X.; Guo, L.F.; Fu, L.L.; Tang, S.F. Study on multi size seed metering device for vertical plate soybean precision planter. *Int. J. Agric. Biol. Eng.* **2015**, *8*, 1–8.
9. Ess, D.R.; Hawkins, S.E.; Young, J.C.; Christmas, E.P. Evaluation of the performance of abelt metering system for soybeans planted with a grain drill. *Appl. Eng. Agric.* **2005**, *6*, 965–969. [CrossRef]

10. Hu, M.J.; Xia, J.F.; Zheng, K.; Du, J.; Liu, Z.Y.; Zhou, M.K. Design and Experiment of Inside-filling Pneumatic High Speed Precision Seed-metering Device for Cotton. *Trans. Chin. Soc. Agric. Mach.* **2021**, *8*, 73–85. (In Chinese with English Abstract)
11. Ni, X.D.; Xu, G.J.; Wang, Q.; Peng, X.R.; Wang, J.; Hu, B. Design and Experiment of Pneumatic Cylinder Array Precision Seed-metering Device for Cotton. *Trans. Chin. Soc. Agric. Mach.* **2017**, *12*, 58–67. (In Chinese with English Abstract)
12. Zhou, Y.; Hu, M.J.; Xia, J.F.; Zhang, G.Z.; Xu, Z.Y.; Feng, C.C.; Tang, N.R.; Liu, D.Z. Design and experiment of inside-filling adjustable precision seed-metering device with combined hole for cotton. *Trans. Chin. Soc. Agric. Eng.* **2018**, *18*, 59–67. (In Chinese with English Abstract)
13. Zhang, X.J.; Chen, Y.; Shi, Z.L.; Jin, W.; Zhang, H.T.; Fu, H.; Wang, D.J. Design and experiment of double-storage turntable cotton vertical disc hole seeding and metering device. *Trans. Chin. Soc. Agric. Eng.* **2021**, *19*, 27–36. (In Chinese with English Abstract)
14. Li, J.J.; Zhang, H.P.; Bi, X.S.; Wang, J.; Hu, B.; Li, S.Z. Simulation analysis and test on the filling performance of rotary type-hole precision seed-metering device for cotton. *Trans. Chin. Soc. Agric. Eng.* **2020**, *5*, 38–49. (In Chinese with English Abstract)
15. Ma, W.P.; You, Y.; Wang, D.C.; Ni, S.J.; Xun, X.L. Parameter Calibration of Alfalfa Seed Discrete Element Model Based on RSM and NSGA-II. *Trans. Chin. Soc. Agric. Mach.* **2020**, *8*, 136–144. (In Chinese with English Abstract)
16. Shi, L.R.; Sun, W.; Zhao, W.Y.; Yang, X.P.; Feng, B. Parameter determination and validation of discrete element model of seed potato mechanical seeding. *Trans. Chin. Soc. Agric. Eng.* **2018**, *6*, 35–42. (In Chinese with English Abstract)
17. Rackl, M.; Hanley, K.J. A methodical calibration procedure for discrete element models. *Powder Technol.* **2017**, *307*, 73–83. (In Chinese with English Abstract) [CrossRef]
18. Coetzee, C.J. Review Calibration of the discrete element method. *Powder Technol.* **2017**, *310*, 104–142. [CrossRef]
19. Liu, R.; Li, Y.J.; Liu, Z.J.; Liu, L.J.; Lv, H.T. Analysis and Calibration of Discrete Element Parameters of Coated Maize Seed. *Trans. Chin. Soc. Agric. Mach.* **2021**, *52*, 1–8. (In Chinese with English Abstract)
20. Liu, W.Z.; He, J.; Li, H.W.; Li, X.Q.; Zheng, K.; Wei, Z.C. Calibration of Simulation Parameters for Potato Minituber Based on EDEM. *Trans. Chin. Soc. Agric. Mach.* **2018**, *5*, 125–135, 142. (In Chinese with English Abstract)
21. Wang, Y.X.; Liang, Z.J.; Zhang, D.X.; Cui, T.; Shi, S.; Li, K.H.; Yang, L. Calibration method of contact characteristic parameters for corn seeds based on EDEM. *Trans. Chin. Soc. Agric. Eng.* **2016**, *22*, 36–42. (In Chinese with English Abstract)
22. Liu, F.Y.; Zhang, J.; Li, B.; Chen, J. Calibration of parameters of wheat required in discrete element method simulation based on repose angle of particle heap. *Trans. Chin. Soc. Agric. Eng.* **2016**, *12*, 247–253. (In Chinese with English Abstract)
23. Lu, F.; Ma, X.; Tan, S.Y.; Chen, L.T.; Zeng, L.C.; An, B. Simulative Calibration and Experiment on Main Contact Parameters of Discrete Elements for Rice Bud Seeds. *Trans. Chin. Soc. Agric. Mach.* **2018**, *2*, 93–99. (In Chinese with English Abstract)
24. Hao, J.J.; Wei, W.B.; Huang, P.C.; Qin, J.H.; Zhao, J.G. Calibration and experimental verification of discrete element parameters of oil sunflower seeds. *Trans. Chin. Soc. Agric. Eng.* **2021**, *12*, 36–44. (In Chinese with English Abstract)
25. Yu, Q.X.; Liu, Y.; Chen, X.B.; Sun, K.; Lai, Q.H. Calibration and Experiment of Simulation Parameters for Panax notoginseng seeds based on DEM. *Trans. Chin. Soc. Agric. Eng.* **2020**, *2*, 123–132. (In Chinese with English Abstract)
26. Hou, Z.F.; Dai, N.Z.; Chen, Z.; Chou, Y.; Zhang, X.W. Measurement and calibration of physical property parameters for Agropyron seeds in a discrete element simulation. *Trans. Chin. Soc. Agric. Eng.* **2020**, *24*, 46–54. (In Chinese with English Abstract)
27. Ma, Y.H. *Agricultural Materials Science*; Chemical Industry Press: Beijing, China, 2015; (In Chinese with English Abstract)
28. Khodabakhshian, R. Poisson's ratio of pumpkin seeds and their kernels as a function of variety, size, moisture content and loading rate. *Agric. Eng. Int. CIGR J.* **2012**, *3*, 203–209.
29. Wang, L.; He, X.W.; Hu, C.; Guo, W.S.; Wang, X.F.; Xing, J.F.; Hou, S.L. Measurement of the physical parameters and calibration of discrete element simulation parameter of coated cotton seed. *J. China Agric. Univ.* **2022**, *6*, 71–82. (In Chinese with English Abstract)
30. Zhang, R.; Han, D.L.; Ji, Q.L.; He, Y.; Li, J.Q. Calibration methods of sandy soil parameters in simulation of discrete element method. *Trans. Chin. Soc. Agric. Mach.* **2017**, *3*, 49–56. (In Chinese with English Abstract)
31. Li, S.N.; Lin, X.; Chen, Y.; Ma, L.Z. 3D converse modeling for sphere point cloud. *J. Graph.* **2013**, *34*, 49–52. (In Chinese with English Abstract)
32. Liu, C.L.; Wang, Y.L.; Song, J.N.; Li, Y.N.; Ma, T. Experiment and discrete element model of rice seed based on 3D laser scanning. *Trans. Chin. Soc. Agric. Eng.* **2016**, *15*, 294–300. (In Chinese with English Abstract)
33. Li, Y.X.; Li, F.X.; Xu, X.M.; Sheng, C.P.; Meng, K.P.; Chen, J.; Chang, D.Q. Parameter calibration of wheat flour for discrete element method simulation based on particle scaling. *Trans. Chin. Soc. Agric. Eng.* **2019**, *16*, 320–327. (In Chinese with English Abstract)
34. Huo, X.C. *The Experimental Research on Discrete Element Analysis Parameters of the Agaricus Bisporus Seeds and the Seed-metering Device Optimization*; Chinese Academy of Agricultural Sciences: Beijing, China, 2019; (In Chinese with English Abstract)
35. Lu, Y.G.; Wu, N.; Wang, B.; Yu, Z.Y.; Lin, D.C.; Hu, Z.C. Measurement and analysis of peanuts' restitution coefficient in point-to-plate collision model. *J. China Agric. Univ.* **2016**, *8*, 111–118. (In Chinese with English Abstract)
36. Ge, T.; Jia, Z.H.; Zhou, K.D. A theoretical model for the coefficient of restitution calculation of point impact. *Mech. Des. Res.* **2007**, *23*, 14–16. (In Chinese with English Abstract).
37. Yu, C.C.; Duan, H.B.; Cai, X.K.; Xu, T.; Yao, F.H.; Chen, Z.H.; Yan, F.Y. Discrete element simulation parameters-based measurement of materials for potato minituber. *J. Huazhong Agric. Univ.* **2021**, *1*, 210–217. (In Chinese with English Abstract)
38. Zhang, S.W.; Zhang, R.Y.; Chen, T.Y.; Fu, Q.; Yuan, H.F. Calibration of Simulation Parameters of Mung-been Seeds Using Discrete Element Method and Verification of Seed-metering Test. *Trans. Chin. Soc. Agric. Mach.* **2022**, *3*, 71–79. (In Chinese with English Abstract)
39. Hamzah, M.; Beakawi, A.H.; Omar, S. A review on the angle of repose of granular materials. *Powder Technol.* **2018**, *330*, 397–417.

40. Tsa, B.; Rf, B.; Er, B. Classification of granular materials via flowability-based clustering with application to bulk feeding. *Powder Technol.* **2021**, *378*, 288–302.
41. Müller, D.; Fimbinger, E.; Brand, C. Algorithm for the determination of the angle of repose in bulk material analysis. *Powder Technol.* **2021**, *383*, 598–605. [CrossRef]
42. Ge, Y.Y. *Experiment Design Method and Application of Design-Expert Software*; Harbin Institute of Technology Press: Harbin, China, 2015; (In Chinese with English Abstract)
43. Fu, J.; Yuan, H.K.; Zhang, D.P.; Chen, Z.; Ren, L.Q. Multi-objective optimization of process parameters of longitudinal axial threshing cylinder for frozen corn using RSM and NSGA-II. *Appl. Sci.* **2020**, *5*, 1646. [CrossRef]